



HAL
open science

Bioinspired surfaces with strong water adhesion by electropolymerization of thieno[3,4-b]thiophene with mixed hydrocarbon/short fluorocarbon chains

El Hadji Yade Thiam, Abdoulaye Dramé, Aboubacary Séne, Salif Sow, Samba Yandé Dieng, Frédéric Guittard, Thierry Darmanin

► To cite this version:

El Hadji Yade Thiam, Abdoulaye Dramé, Aboubacary Séne, Salif Sow, Samba Yandé Dieng, et al.. Bioinspired surfaces with strong water adhesion by electropolymerization of thieno[3,4-b]thiophene with mixed hydrocarbon/short fluorocarbon chains. *Journal of Fluorine Chemistry*, 2020, 10.1016/j.jfluchem.2020.109574 . hal-03554128

HAL Id: hal-03554128

<https://hal.science/hal-03554128>

Submitted on 3 Feb 2022

HAL is a multi-disciplinary open access archive for the deposit and dissemination of scientific research documents, whether they are published or not. The documents may come from teaching and research institutions in France or abroad, or from public or private research centers.

L'archive ouverte pluridisciplinaire **HAL**, est destinée au dépôt et à la diffusion de documents scientifiques de niveau recherche, publiés ou non, émanant des établissements d'enseignement et de recherche français ou étrangers, des laboratoires publics ou privés.

Bioinspired surfaces with strong water adhesion by electropolymerization of thieno[3,4-*b*]thiophene with mixed hydrocarbon/short fluorocarbon chains

El hadji Yade Thiam,^a Abdoulaye Dramé,^a Aboubacary Séné,^a Salif Sow,^a Samba Yandé Dieng,^a Frédéric Guittard^{b,c} and Thierry Darmanin^{b,*}

^a*Université Cheikh Anta Diop, Faculté des Sciences et Techniques, Département de Chimie, B.P. 5005 Dakar, Sénégal.*

^b*Université Côte d'Azur, NICE Lab, IMREDD, 61-63 Av. Simon Veil, 06200 Nice, France.*

Corresponding author: thierry.darmanin@unice.fr

^c*University California Riverside, Department of Bioengineering, Riverside, CA, USA*

Abstract

Here, in the aim to replace long perfluorinated chains (C₈F₁₇) in polymer we use both a short C₄F₉ perfluorinated chain and a hydrocarbon chain a various length (from C₂ to C₁₂). These chains are grafted to thieno[3,4-*b*]thiophene monomers to perform electrodeposited conducting polymer films with high hydrophobic properties. Two solvents are used: dichloromethane (CH₂Cl₂) and dichloromethane saturated with water (CH₂Cl₂ + H₂O) in order to release also *in-situ* O₂ and/ or H₂ gas bubbles. In CH₂Cl₂, spherical particles covering the surface are observed with short alkyl chains and large wrinkles with long alkyl chains. The highest hydrophobicity $\theta_w = 139.3^\circ$ are obtained with Thieno-F₄-C₆ after 5 deposition scans, which presents also strong water adhesion. In CH₂Cl₂ + H₂O, the surfaces are smoother and traces of very large bubbles are present but only with short alkyl chains. However, the polymer growth is inhomogeneous because the substituents are too flexible to stabilize the released gas bubbles. The preliminary results are encouraging and more rigid substituents or spacers could be envisaged in the future to induce homogenous porous structures.

Keywords: Wettability, Parahydrophobic, Electropolymerization, Conducting polymers, Bioinspiration

1. Introduction

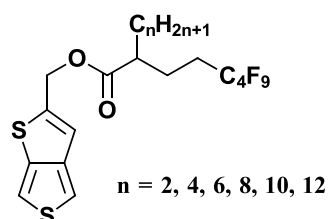
The bio-inspiration is an excellent way to perform a breakthrough in a scientific field [1–4] and this is especially true in the wetting properties [5–8]. In Nature, many species display surfaces with special wettability by using textured surfaces [9,10]. For example, it exists species with ultra-low water adhesion such as the “lotus-effect” (superhydrophobic) and other with very-high water adhesion such as the “petal-effect” (parahydrophobic) [11–14]. These surface properties are highly dependent on the surface energy and the surface roughness/structuring. Controlling the two key parameters is fundamental for various applications such as in optical devices, anti-fogging/anti-icing substrates or in oil/water separation membranes [15–18].

The electropolymerization is an excellent and quick process to prepare surfaces with controlled surface energy and surface roughness. In this process, a monomer is oxidized to induce the formation of a conducting polymer film of various roughness on a working electrode [19–22]. It is known conducting polymers can self-assemble to obtain structures of various shapes such as fibers, sheets or spherical particles, as observed with aniline [23,24]. Substituents can also be grafted, for example on the monomer structure [25–27]. In order to highly reduce the surface energy, long perfluorinated chains such as perfluorooctyl chains (C_8F_{17}) are often used to increase the hydrophobic/oleophobic properties. However, due to persistence in the environment (bioaccumulative potential), the industries have to replace them in a relatively short time [28,29]. It was shown that shorter fluorinated chains such as perfluorobutyl (C_4F_9), seem to have lower bioaccumulative potential [30–32].

In the case of electrodeposited polymers, it was shown that short C_4F_9 chains can give in certain conditions better results than long C_8F_{17} chains because the fluorinated chain length has also an influence on the surface morphology. It was the case of 3,4-ethylenedioxythiophene (EDOT) for which nanofibers were obtained with C_4F_9 chains and cauliflower-like structures with C_8F_{17} chains. Short fluorinated chains (C_4F_9) can also be mixed with hydrocarbon chains in order to increase the surface hydrophobicity even if the surface oleophobicity is expected to decrease.

Very recently, it was shown that thieno[3,4-*b*]thiophene are excellent candidates to obtain structured surfaces [33–37]. Here, we investigate original thieno[3,4-*b*]thiophene with mixed hydrocarbon/short fluorocarbon chains in aim but to reduce the bioaccumulative potential of polymers with long fluorocarbon chains. Hydrocarbon chains of various length (from C_2 to C_{12}) are used. Because, it was also reported the possibility to obtain porous structures by

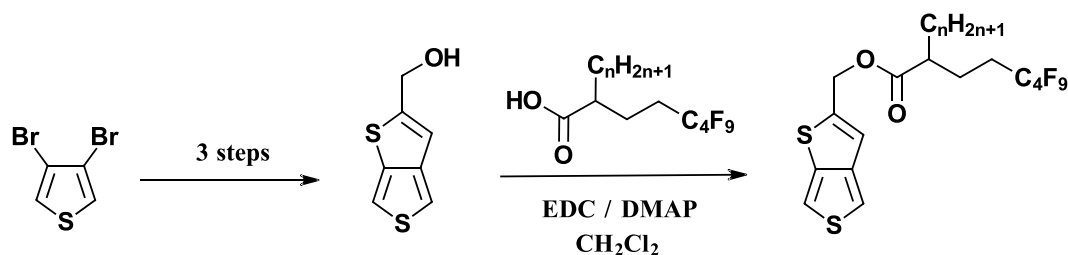
adding water in solution which can release O₂ and/ or H₂ gas bubbles (templateless electropolymerization) [35], here two solvents are tested: dichloromethane (CH₂Cl₂) and dichloromethane saturated with water (called here CH₂Cl₂ + H₂O).



Scheme 1. Monomers investigated in this work.

2. Experimental Section

2.1. Monomer synthesis



Scheme 2. Chemical route to the monomers.

The chemical way is schematized in Scheme 2. Here, the acids with both fluorinated and alkyl chains were synthesized using a procedure reported in the literature [38–40]. Then, the monomers were synthesized by esterification. 1.2 eq. of the corresponding carboxylic acid, 1.2 eq. 130 g of *N*-(3-dimethylaminopropyl)-*N'*-ethylcarbodiimide hydrochloride (130 mg) and 4-(dimethylamino)pyridine (DMAP) (20 mg) were added to 20 mL of dichloromethane. After stirring for 30 min, 100 mg of Thieno-OH (1eq.) [41–43] was added to the mixture. After one day, the crude product was purified by column chromatography (silica gel, eluent cyclohexane : diethyl ether).

Thieno-F₄-C₂: Thieno[3,4-*b*]thiophen-2-ylmethyl 2-ethyl-5,5,6,6,7,7,8,8,8-nonafluorooctanoate. Yield 47%; Liquid; δ_{H} (200 MHz, CDCl₃): 7.30 (d, $J = 2.80$ Hz, 1H), 7.21 (dd, $J = 2.4$ Hz, $J = 0.7$ Hz, 1H), 6.88 (s, 1H), 5.18 (m, 2H); 2.51 (m, 1H); 1.91 (m, 4H); 1.60 (m, 2H); 0.89 (t, $J = 6.6$ Hz, 3H); δ_{C} (200 MHz, CDCl₃): 174.61, 146.35, 144.62, 139.96,

117.91, 112.52, 110.62, 62.16, 46.13, 32.22, 31.75, 29.14, 27.77, 25.36, 22.07, 14.61; MS (70 eV): m/z 486 (M^+ , 17), 170 ($C_7H_6OS_2$, 100).

Thieno-F4-C4: Thieno[3,4-*b*]thiophen-2-ylmethyl 2-butyl-5,5,6,6,7,7,8,8,8-nonafluorooctanoate. Yield 44%; Liquid; δ_H (200 MHz, $CDCl_3$): 7.31 (d, $J = 2.8$ Hz, 1H), 7.22 (dd, $J = 2.4$ Hz, $J = 0.7$ Hz, 1H), 6.90 (s, 1H), 5.27 (m, 2H); 2.51 (m, 1H); 2.01 (m, 2H); 1.80 (m, 2H); 1.61 (m, 2H); 1.30 (m, 4H); 0.90 (t, $J = 6.5$ Hz, 3H); δ_C (200 MHz, $CDCl_3$): 174.46, 146.04, 144.29, 138.80, 117.16, 112.59, 110.69, 61.55, 44.05, 31.39, 29.70, 22.99, 14.32; MS (70 eV): m/z 514 (M^+ , 10), 170 ($C_7H_6OS_2$, 100).

Thieno-F4-C6: Thieno[3,4-*b*]thiophen-2-ylmethyl 5,5,6,6,7,7,8,8,8-nonafluoro-2-hexyloctanoate. Yield 63%; Crystalline solid; m.p. 32.6°C; δ_H (200 MHz, $CDCl_3$): 7.30 (d, $J = 2.7$ Hz, 1H), 7.21 (dd, $J = 2.3$ Hz, $J = 0.6$ Hz, 1H), 6.88 (s, 1H), 5.17 (m, 2H); 2.51 (m, 1H); 1.91 (m, 4H); 1.61 (m, 2H); 1.30 (m, 8H); 0.89 (t, $J = 6.5$ Hz, 3H); δ_C (200 MHz, $CDCl_3$): 174.67, 146.24, 144.49, 139.01, 117.39, 112.79, 110.87, 62.01, 44.58, 32.22, 31.55, 29.04, 26.99, 26.90, 22.49, 14.00; MS (70 eV): m/z 542 (M^+ , 13), 170 ($C_7H_6OS_2$, 100).

Thieno-F4-C8: Thieno[3,4-*b*]thiophen-2-ylmethyl 2-(3,3,4,4,5,5,6,6,6-nonafluorohexyl)decanoate. Yield 40%; Crystalline solid; m.p. 15.4°C; δ_H (200 MHz, $CDCl_3$): 7.31 (d, $J = 2.7$ Hz, 1H), 7.22 (dd, $J = 2.4$ Hz, $J = 0.7$ Hz, 1H), 6.90 (s, 1H), 5.17 (m, 2H); 2.50 (m, 1H); 1.90 (m, 4H); 1.61 (m, 2H); 1.30 (m, 12H); 0.87 (t, $J = 6.5$ Hz, 3H); δ_C (200 MHz, $CDCl_3$): 174.82, 146.38, 144.64, 139.15, 117.52, 112.94, 111.02, 62.17, 44.71, 32.36, 31.95, 29.53, 29.46, 29.29, 28.74, 27.19, 22.76, 22.59, 22.52, 14.23; MS (70 eV): m/z 570.1 (M^+ , 13), 170 ($C_7H_6OS_2$, 100).

Thieno-F4-C10: Thieno[3,4-*b*]thiophen-2-ylmethyl 2-(3,3,4,4,5,5,6,6,6-nonafluorohexyl)dodecanoate. Yield 32%; Liquid; δ_H (200 MHz, $CDCl_3$): 7.31 (d, $J = 2.8$ Hz, 1H), 7.22 (dd, $J = 2.4$ Hz, $J = 0.7$ Hz, 1H), 6.90 (s, 1H), 5.17 (m, 2H); 2.50 (m, 1H); 2.00 (m, 6H); 1.30 (m, 16H); 0.87 (t, $J = 6.5$ Hz, 3H); δ_C (200 MHz, $CDCl_3$): 174.04, 146.60, 144.86, 139.37, 117.73, 112.16, 110.24, 62.39, 44.93, 32.58, 32.26, 29.92, 29.86, 29.73, 29.66, 28.97, 27.41, 23.04, 22.81, 22.46, 14.21; MS (70 eV): m/z 598.1 (M^+ , 07), 170 ($C_7H_6OS_2$, 100).

Thieno-F4-C12: Thieno[3,4-*b*]thiophen-2-ylmethyl 2-(3,3,4,4,5,5,6,6,6-nonafluorohexyl)tetradecanoate. Yield 33%; Crystalline solid; m.p. 15.4°C; δ_H (200 MHz, $CDCl_3$): 7.32 (d, $J = 2.9$ Hz, 1H), 7.23 (dd, $J = 2.5$ Hz, $J = 0.8$ Hz, 1H), 6.89 (s, 1H), 5.17 (m, 2H); 2.50 (m, 1H); 2.00 (m, 6H); 1.30 (m, 20H); 0.87 (t, $J = 6.5$ Hz, 3H); δ_C (200 MHz, $CDCl_3$): 174.67, 146.24, 144.50, 139.01, 117.37, 112.79, 110.87, 62.02, 44.57, 32.21, 31.91,

29.63, 29.50, 29.35, 28.60, 27.05, 22.68, 22.45, 22.46, 14.10; MS (70 eV): m/z 626.1 (M^+ , 18), 170 ($C_7H_6OS_2$, 100).

2.2. Surface preparation

The conducting polymer surfaces were obtained by electropolymerization using an Autolab potentiostat (Metrohm). 2 cm² gold-coated silicon wafers were used to deposit the polymers. A carbon rod was used as the counter-electrode and a saturated calomel electrode as the reference electrode. The electrolyte used was tetrabutylammonium (Bu_4NClO_4) diluted (0.1 M) in either dichloromethane (CH_2Cl_2) or dichloromethane saturated in water called here ($CH_2Cl_2 + H_2O$). For the last one, deionized H_2O was added to CH_2Cl_2 and the highly mixed. Then, the remaining H_2O was removed by extraction. The modified substrates were finally washed three times in CH_2Cl_2 and slowly dried.

2.3. Surface characterization

The surface morphology was characterized by scanning electron microscopy (SEM) using a 6700F microscope (JEOL). For the surface wetting properties, DSA30 goniometer (Bruker) was used. The water apparent contact angles (θ_w) were determined by depositing 2 μ L water droplets on the substrates. The angles were determined at the triple point. Each data given here is a mean of five measurements.

3. Results and Discussion

First, the two studied solvents (CH_2Cl_2 and $CH_2Cl_2 + H_2O$) were electrochemically characterized by cyclic voltammetry (Figure 1), especially for evaluating H_2O presence. 0.1 M of Bu_4NClO_4 was used as the electrolyte. Using $CH_2Cl_2 + H_2O$, a very intense peak for H_2 formation ($2 H_2O + 2 e^- \rightarrow H_2 + 2OH^-$) is present between 0 and -1 V vs SCE only during the back scan. For O_2 formation ($2 H_2O \rightarrow O_2 + 4H^+ + 4 e^-$), a peak is present during the forward scan but starts only at ≈ 2 V vs SCE. Then, the monomers were added and the monomer oxidation potential (E^{ox}) were determined at 1.68–1.71 V vs SCE.

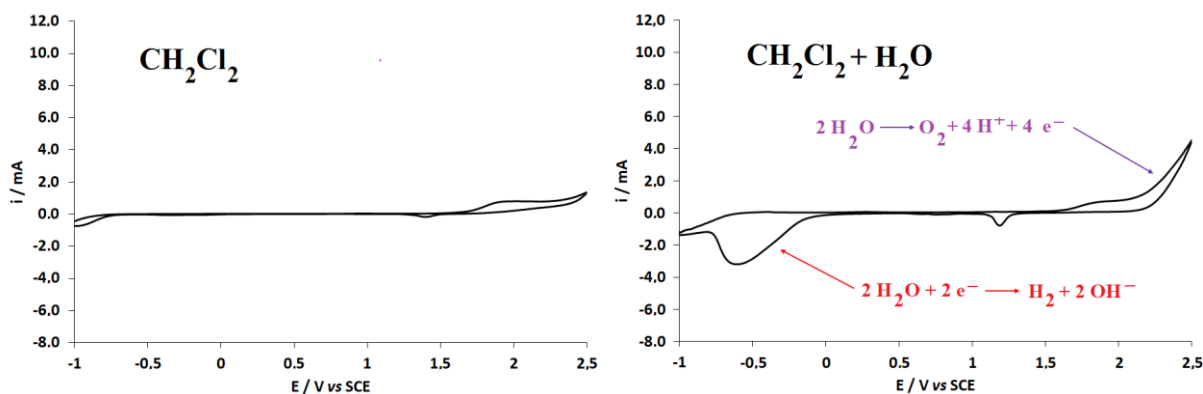


Figure 1. Cyclic voltammograms (1 scan) of the solvents CH_2Cl_2 (left column) and $\text{CH}_2\text{Cl}_2 + \text{H}_2\text{O}$ (right column) with Bu_4NClO_4 as electrolyte. Scan rate: 20 mV s^{-1} .

Then, the polymers were electrodeposited by cyclic voltammetry from -1 V to E^{ox} in the two different solvents (CH_2Cl_2 and $\text{CH}_2\text{Cl}_2 + \text{H}_2\text{O}$). With this potential range, especially H_2 bubbles are expected. Some of the cyclic voltammograms are given in Figure 2 but we observed the same tendency. For Thieno- $\text{F}_4\text{-C}_2$ electrodeposited in CH_2Cl_2 , we observed very intense peaks due to the presence of the polymer films. The oxidation peaks are present at $\approx 0.45 \text{ V}$ during the forward scans and the reduction peaks at $\approx 0.10 \text{ V}$ during the back scans. It should also be noticed the presence of multiple peaks especially visible in the cyclic voltammograms during the back indicating their ability to sustain multiple oxidation/reduction steps. It is also observed that the intensity of these peaks decreases when the alkyl chain length increases from Thieno- $\text{F}_4\text{-C}_2$ to Thieno- $\text{F}_4\text{-C}_{12}$. By contrast, the cyclic voltammograms in $\text{CH}_2\text{Cl}_2 + \text{H}_2\text{O}$ are extremely different. For example, for Thieno- $\text{F}_4\text{-C}_2$ electrodeposited in $\text{CH}_2\text{Cl}_2 + \text{H}_2\text{O}$ we observe first a very huge decrease of the intensity of the polymer peaks. However, a novel peak at $\approx -0.75 \text{ V}$ is present but only during the back scans. It was shown that this peak is probably due the formation of H_2 bubbles from H_2O ($2 \text{ H}_2\text{O} + 2 \text{ e}^- \rightarrow \text{H}_2 \text{ (bubbles)} + 2 \text{ OH}^-$) and this is why it is especially present in $\text{CH}_2\text{Cl}_2 + \text{H}_2\text{O}$ [33].

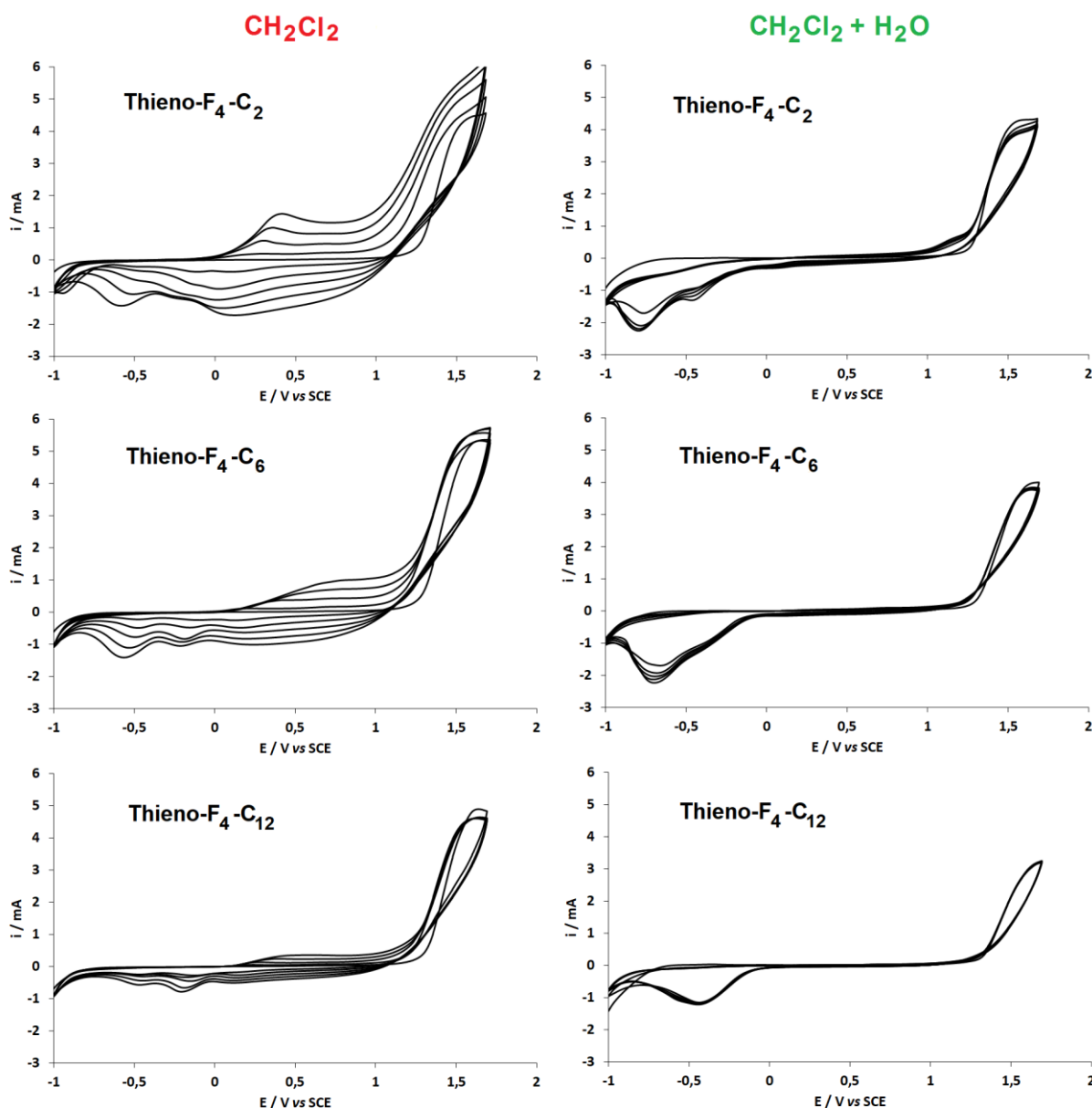


Figure 2. Electropolymerization curves of some of the monomers (0.01 M) in CH_2Cl_2 or $\text{CH}_2\text{Cl}_2 + \text{H}_2\text{O}$ / Bu_4NClO_4 (0.1 M); 5 scans at a scan rate of 20 mV s^{-1} .

The SEM images are given in Figure 3 and the surface properties are gathered in Table 1 and Table 2. Using CH_2Cl_2 , the films formed with Thieno-F₄-C₂ are rough and composed of spherical particles. The surfaces are highly hydrophobic with $\theta_w = 136.7$ after 3 deposition scans. When the alkyl chain length increases from C₂ to C₁₂, it is expected that the surface energy decreases. However, at the same time, it is observed a decrease in the number of spherical particles even if some large wrinkles also appear, which can also affect the surface hydrophobicity. This is expected because it was shown in the literature that the surface roughness can highly decrease if the polymer solubility increases. After, in a solvent of low

polarity such as CH_2Cl_2 , it is expected that the polymer solubility increases with the alkyl chain length. Hence, the highest $\theta_w = 139.3$ are obtained with Thieno-F4-C₆ after 5 deposition scans. Moreover, the water droplets remain stuck on the surface even with a substrate inclination of 90° (Figure 4), indicating of parahydrophobic properties, as observed on rose petals [11-13].

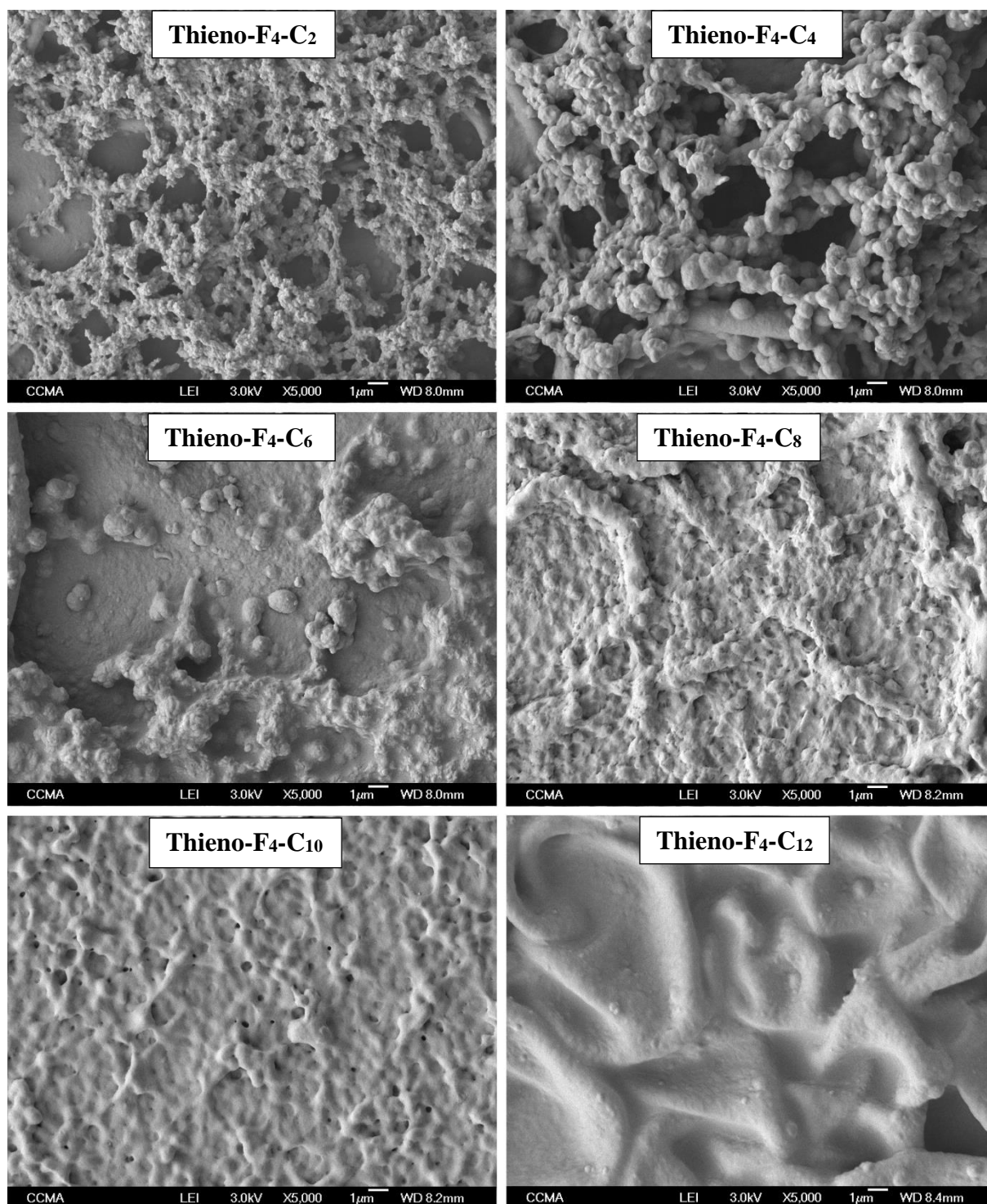


Figure 3. SEM images of polymer surfaces obtained from Thieno-F₄-C₂, Thieno-F₄-C₄, Thieno-F₄-C₆, Thieno-F₄-C₈, Thieno-F₄-C₁₀ and Thieno-F₄-C₁₂ with the solvent CH₂Cl₂ and by cyclic voltammetry (3 scans).

Table 1. Roughness (Ra and Rq) and wettability data for the polymer films obtained in CH₂Cl₂.

Polymer	Number of deposition scans	Ra [nm]	Rq [nm]	θ_w [deg]
Thieno-F ₄ -C ₂	1	101 ± 66	136 ± 94	51.2 ± 4.4
	3	134 ± 51	182 ± 65	136.7 ± 3.7
	5	300 ± 56	437 ± 83	127.5 ± 3.1
Thieno-F ₄ -C ₄	1	42 ± 45	57 ± 61	86.1 ± 7.9
	3	320 ± 17	420 ± 25	127.5 ± 10.6
	5	616 ± 48	877 ± 55	131.7 ± 3.1
Thieno-F ₄ -C ₆	1	20 ± 5	27 ± 7	99.4 ± 1.4
	3	151 ± 96	412 ± 275	131.9 ± 4.1
	5	312 ± 10	423 ± 20	139.3 ± 8.4
Thieno-F ₄ -C ₈	1	62 ± 27	85 ± 43	102.1 ± 7.5
	3	214 ± 42	286 ± 45	125.7 ± 6.1
	5	166 ± 61	239 ± 66	124.8 ± 16.4
Thieno-F ₄ -C ₁₀	1	90 ± 37	119 ± 43	90.9 ± 11.1
	3	273 ± 136	362 ± 191	119.3 ± 4.1
	5	201 ± 95	282 ± 17	124.7 ± 4.1
Thieno-F ₄ -C ₁₂	1	301 ± 30	447 ± 46	102.7 ± 1.0
	3	245 ± 86	323 ± 103	117.8 ± 9.8
	5	210 ± 133	268 ± 168	119.6 ± 10.5

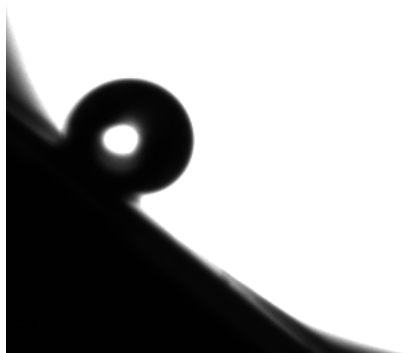


Figure 4. Picture of a water droplet on poly(**Thieno-F4-C6**) (5 scans) coated-substrate with an inclination of 45° .

Using $\text{CH}_2\text{Cl}_2 + \text{H}_2\text{O}$, the surfaces are less rough and the large wrinkles are no more present (Figure 5). The traces of very large bubbles are clearly visible on the surfaces meaning that polymers grew around them. But the polymer growth is inhomogeneous. This is not surprising because it was shown that the polymer rigidity is a very important parameter to obtain homogeneous porous surfaces. Here, the substituents used are too flexible. This is why also, we clearly observe the disappearances of traces of these large bubbles as the alkyl chain increases until to be completely smooth for Thieno-F₄-C₁₂. Hence, the highest $\theta_w = 115.4$ are obtained with Thieno-F₄-C₈ after 5 deposition scans.

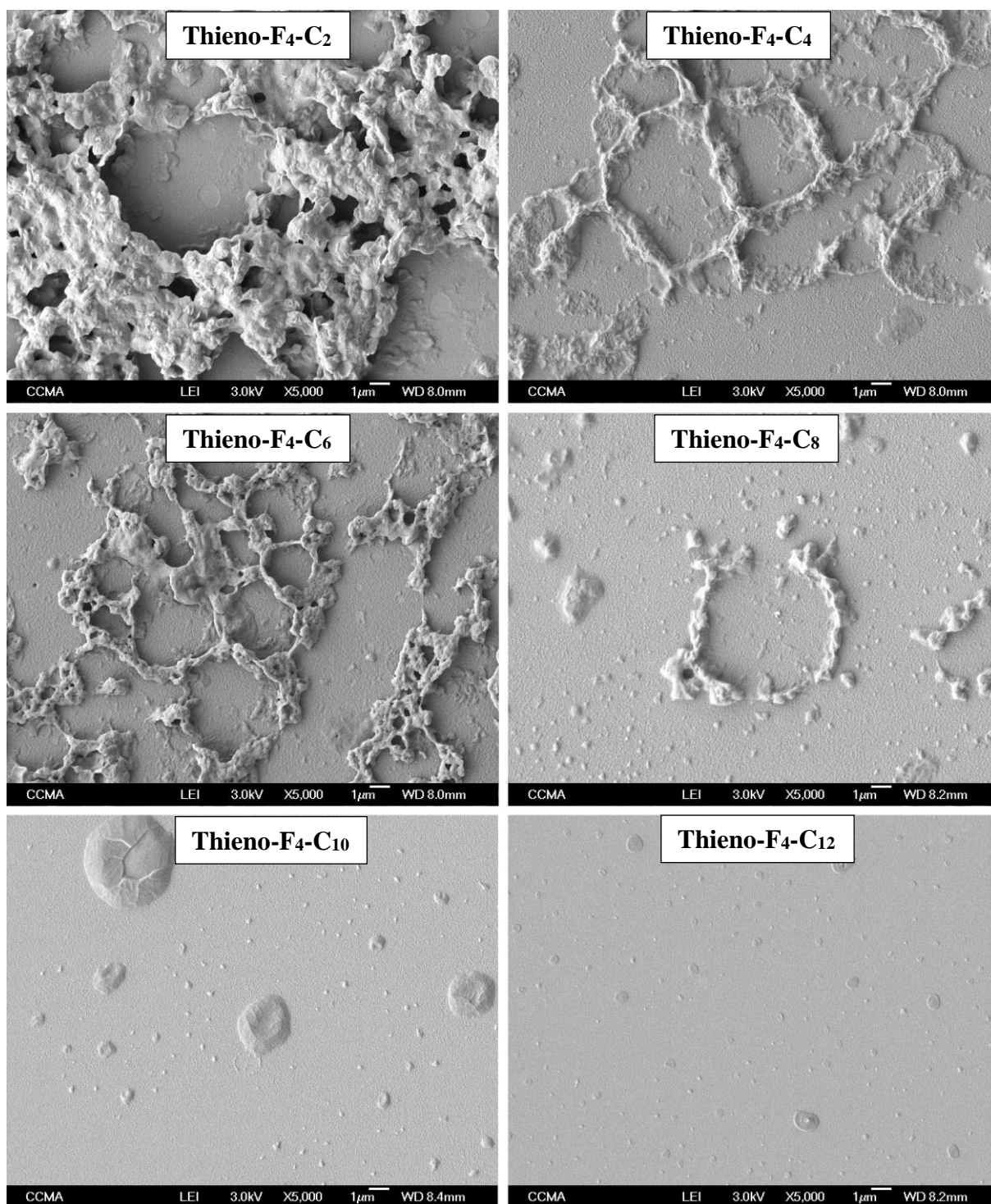


Figure 5. SEM images of polymer surfaces obtained from Thieno-F₄-C₂, Thieno-F₄-C₄, Thieno-F₄-C₆, Thieno-F₄-C₈, Thieno-F₄-C₁₀ and Thieno-F₄-C₁₂ with the solvent CH₂Cl₂ + H₂O and by cyclic voltammetry (3 scans).

Table 2. Roughness (Ra and Rq) and wettability data for the polymer films obtained in CH₂Cl₂ + H₂O.

Polymer	Number of deposition scans	Ra [nm]	Rq [nm]	θ_w [deg]
Thieno-F ₄ -C ₂	1	234 ± 45	360 ± 90	86.8 ± 8.3
	3	120 ± 13	185 ± 42	98.2 ± 7.2
	5	162 ± 40	254 ± 46	109.3 ± 6.7
Thieno-F ₄ -C ₄	1	53 ± 29	91 ± 62	87.6 ± 7.4
	3	90 ± 45	175 ± 89	84.4 ± 1.9
	5	193 ± 73	301 ± 144	91.6 ± 5.9
Thieno-F ₄ -C ₆	1	49 ± 23	67 ± 37	85.4 ± 8.2
	3	105 ± 14	160 ± 35	81.9 ± 3.8
	5	224 ± 39	338 ± 38	105.2 ± 10.8
Thieno-F ₄ -C ₈	1	28 ± 8	50 ± 18	100.9 ± 1.3
	3	70 ± 12	126 ± 31	91.6 ± 2.0
	5	107 ± 36	143 ± 41	115.4 ± 6.3
Thieno-F ₄ -C ₁₀	1	33 ± 8	58 ± 26	99.0 ± 2.7
	3	42 ± 5	55 ± 7	102.5 ± 0.7
	5	51 ± 8	75 ± 15	105.7 ± 0.9
Thieno-F ₄ -C ₁₂	1	56 ± 22	103 ± 67	99.8 ± 5.0
	3	42 ± 4	61 ± 10	103.2 ± 0.6
	5	66 ± 10	101 ± 10	104.0 ± 1.2

4. Conclusion

Here, we have shown the possibility to replace long perfluorinated C₈F₁₇ chains by both a short C₄F₉ perfluorinated chain and a hydrocarbon chain a various length (from C₂ to C₁₂) in order to obtain very interesting hydrophobic properties. By grafting them onto thieno[3,4-*b*]thiophene monomers, electrodeposited conducting polymer films were studied in two solvents: CH₂Cl₂ and CH₂Cl₂ + H₂O in order to release *in-situ* O₂ and/ or H₂ gas bubbles. In CH₂Cl₂, the highest hydrophobicity $\theta_w = 139.3^\circ$ were observed with Thieno-F₄-C₆ after 5 deposition scans. Spherical particles were observed rather with short alkyl chains and large wrinkles with long alkyl chains. In CH₂Cl₂ + H₂O, the surfaces were smoother and traces of very large bubbles were observed only with short alkyl chains. The inhomogeneity of the polymer growth can be explained by the high substituent flexibility impeding the stabilization of the released gas bubbles. The results are extremely interesting and more rigid substituents or spacers could be envisaged in the future to induce homogenous porous structures.

References

- [1] V.I. Vullev, J. Phys. Chem. Lett. 2 (2011) 503–508.
- [2] T. Hu, L. Li, J. Zhang, ACS Sustainable Chem. Eng. 6 (2018) 11222–11227.
- [3] F. Pina, J. Agric. Food Chem. 62 (2014) 6885–6897.
- [4] L. Sun, Y. Huang, Z. Bian, J. Petrosino, Z. Fan, Y. Wang, K.H. Park, T. Yue, M. Schmidt, S. Galster, J. Ma, H. Zhu, M. Zhang, ACS Appl. Mater. Interfaces 8 (2016) 2423–2434.
- [5] B. Su, Y. Tian, L. Jiang, J. Am. Chem. Soc. 138 (2016) 1727–1748.
- [6] S. Yu, Z. Guo, W. Liu, Chem. Commun. 51 (2015) 1775–1794.
- [7] L. Zhang, J. Wu, Y. Wang, Y. Long, N. Zhao, J. Xu, J. Am. Chem. Soc. 134 (2012) 9879–9881.
- [8] Y. Wang, X. Li, H. Hu, G. Liu, M. Rabnawaz, J. Mater. Chem. A 2 (2014) 8094–8102.
- [9] T. Darmanin, F. Guittard, Mater. Today 18 (2015) 18, 273–285.
- [10] W. Barthlott, M. Mail, B. Bhushan, K. Koch, Nano-Micro Lett. 9 (2017) 23.
- [11] A. Marmur, Soft Matter 8 (2012) 6867–6870.
- [12] C.R. Szczepanski, T. Darmanin, F. Guittard, Adv. Colloid Interface Sci. 241 (2017) 37–61.

- [13] L. Feng, Y. Zhang, J. Xi, Y. Zhu, N. Wang, F. Xia, L. Jiang, *Langmuir* 24 (2008) 4114–4119.
- [14] B. Bhushan, M. Nosonovsky, *Phil. Trans. R. Soc. A* 368 (2010) 4713–4728.
- [15] Y. Cheng, H. Yang, Y. Yang, J. Huang, K. Wu, Z. Chen, X. Wang, C. Lin, Y. Lai, *J. Mater. Chem. B* 6 (2018) 1862–1886.
- [16] B. Li, L. Wu, L. Li, S. Seeger, J. Zhang, A. Wang, *ACS Appl. Mater. Interfaces* 6 (2014) 11581–11588.
- [17] H. Hu, G. Liu, J. Wang, *J. Mater. Chem. A* 7 (2019) 1519–1528.
- [18] J. Yong, F. Chen, Q. Yang, Z. Jiang, X. Hou, *Adv. Mater. Interfaces* 5 (2018) 1701370.
- [19] S. Roquet, P. Leriche, I. Perepichka, B. Jousset, E. Levillain, P. Frère, J. Roncali, *J. Mater. Chem.* 14 (2004) 1396–1400.
- [20] P. Schottland, K. Zong, C.L. Gaupp, B.C. Thompson, C.A. Thomas, I. Giurgiu, R. Hickman, K.A. Abboud, J.R. Reynolds, *Macromolecules* 33 (2000) 7051–7061.
- [21] H.-A. Lin, S.-C. Luo, B. Zhu, C. Chen, Y. Yamashita, H.-h. Yu, *Adv. Funct. Mater.* 23 (2013) 3212–3219.
- [22] A. Çağlar, M. Yıldırım, U. Cengiz, I. Kaya, *Thin Solid Films* 619 (2016) 187–194.
- [23] Y. Zhao, J. Stejskal, J. Wang, *Nanoscale* 5 (2013) 2620–2626.
- [24] Y. Zhu, D. Hu, M.X. Wan, L. Jiang, Y. Wei, *Adv. Mater.* 19 (2007) 2092–2096.
- [25] T. Darmanin, G. Godeau, F. Guittard, E.L. Klimareva, I. Schewtschenko, I.F. Perepichka, *ChemNanoMat* 4 (2018) 656–662.
- [26] G. Ramos Chagas, G. Morán Cruz, R. Méallet-Renault, A. Anne Gaucher, D. Prim, D.E. Weibel, S. Amigoni, F. Guittard, T. Darmanin, *React. Funct. Polym.* 135 (2019) 65–76.
- [27] O. Sane, A. Diouf, S. Y. Dieng, F. Guittard, T. Darmanin, *ChemPlusChem* 83 (2018) 968–975.
- [28] C.A. Ng, K. Hungerbühler, *Environ. Sci. Technol.* 48 (2014) 4637–4648.
- [29] M. Fernández-Sanjuan, M. Faria, S. Lacorte, C. Barata, *Environ. Sci. Pollut. Res.* 20 (2013) 2661–2669.
- [30] J.P. Giesy, K. Kannan, *Environ. Sci. Technol.* 35 (2001) 1339–1342
- [31] N. Kudo, Y. Kawashima, *J. Toxicol. Sci.* 28 (2003) 49–57.
- [32] M. Houde, J.W. Martin, R.J. Letcher, K.R. Solomon, D.C.G. Muir, *Environ. Sci. Technol.* 40 (2006) 3463–3473.
- [33] O. Sane, A. Diouf, G. Morán Cruz, F. Savina, R. Méallet-Renault, S. Amigoni, S.Y. Dieng, F. Guittard, T. Darmanin, *Mater. Today*, 2019, 31, 119–120.
- [34] G. Ramos Chagas, T. Darmanin, G. Godeau, F. Guittard, *Electrochim. Acta* 269 (2018) 462–478.

- [35] G. Ramos Chagas, F. Guittard, T. Darmanin, *ACS Appl. Mater. Interfaces* 8 (2016) 22732–22743.
- [36] G. Ramos Chagas, R. Akbari, G. Godeau, M. Mohammadizadeh, F. Guittard, T. Darmanin, *ChemPlusChem* 82 (2017) 1351–1358.
- [37] O. Thiam, A. Diouf, D. Diouf, S.Y. Dieng, F. Guittard, T. Darmanin, *Phil. Trans. R. Soc. A* 377 (2019) 20190123.
- [38] P. Lucas, M.A. Jouani, H. Trabelsi, A. Cambon, *J. Fluorine Chem.* 92 (1998) 17–22.
- [39] E.Y. Thiam, A. Dramé, A. Sene, S.Y. Dieng, F. Guittard, T. Darmanin, *Eur. Polym. J.* 110 (2019) 76–84.
- [40] J. El-Maiss, T. Darmanin, E. Taffin de Givenchy, S. Amigoni, J. Eastoe, M. Sagisaka, F. Guittard, *J. Polym. Sci., Part B: Polym. Phys.* 52 (2014) 782–788.
- [41] G. Buemi, *Bull. Chem. Soc. Jpn.* 62 (1989) 1262–1268.
- [42] Y. Wada, Y. Asada, T. Ikai, K. Maeda, T. Kuwabara, K. Takahashi, S. Kanoh, *ChemistrySelect* 1 (2016) 703–709.
- [43] P.D. Homyak, J. Tinkham, P.M. Lahti, E.B. Coughlin, *Macromolecules* 46 (2013) 8873–8881.